Proceedings of the Second International Conference on Press-in Engineering 2021, Kochi, Japan – Matsumoto et al (eds)
© 2021 Taylor & Francis Group, London, ISBN 978-1-032-10414-0

A study on the effect an earth-retaining wall's rigidity and embedded depth on its behavior

N. Matsumoto & H. Nishioka
Chuo University, Tokyo, Japan

ABSTRACT: In the design of an earth-retaining cantilever, it is necessary to establish the balance between the retaining wall's rigidity and its embedded depth. In this study, an experiment was conducted using an aluminum-layered ground model that could easily simulate ground failure; the main parameters considered were the rigidity and embedded depth (wall length) of a cantilever-type earth-retaining wall. We demonstrated that highly rigid earth-retaining walls built using traditional design standards are susceptible to brittle collapse. Therefore, the safety against collapse may be improved by increasing the embedding length.

1 INTRODUCTION

For ground excavation using the earth-retaining wall in a neighboring construction site, the displacement of the wall should be limited to minimize its influence on the integrity of the surrounding ground. Therefore, in such cases, the bracing method is generally preferred to the cantilever method. However, to ensure workability inside the excavation, the cantilever method may be adopted by increasing the rigidity of the earth-retaining wall and eliminating the need for struts. In the design for this case, a balance between the rigidity of the earth-retaining wall and the embedded depth must be reasonably established. In some design standards, the embedded depth of the earth-retaining wall should be a depth that can be regarded as a semi-infinite length of the pile. According to this principle, the embedded depth must also be increased as the rigidity of the earth retaining wall increases. However, this may not necessarily result in rational design.

In addition, only a few studies have been conducted wherein the behavior leading up to collapse was simulated using both rigidity and embedded depth as parameters.

Therefore, in this study, we experimented using an aluminum-layered ground model, which can easily simulate failure and subsequent collapse. The main parameters considered were the rigidity and embedded depth (wall length) of the cantilever-type earth-retaining wall.

We also investigated the effects of these parameters on the safety of the cantilever-type earth-retaining wall in terms of collapse and allowable deformation.

2 EXPERIMENT OUTLINE

2.1 *Ground model and experimental equipment*

Two types of aluminum rods with diameters of 3.0 mm and 1.6 mm shown in Figure 1 were used in this experiment. The aluminum-layered ground model was made by mixing these rods well and layered them 40% and 60% in weight content, respectively.

The ground model's weight per unit volume γ and angle of internal friction φ was measured using a measuring box (width = 250 mm and depth 50 = mm). Here, the angle at which the measuring box was tilted and the aluminum rod collapsed (Figures 2 and 3) was defined as the angle of internal friction φ. After three iterations, the average values of $\gamma = 21.0$ kN/m^3 and $\varphi = 30$ ° were obtained.

The ground model was created in an experimental container with a width of 500 mm and a depth of 300 mm, as shown in Figure 4.

In addition, to observe the slip surface in the ground model, horizontal lines were drawn on the end face of the aluminum rod at intervals of 20 mm.

2.2 *Earth-retaining-wall model*

The earth-retaining wall was simulated by inserting a 70-mm-wide aluminum plate into the center of the ground model. There were nine experimental cases involving three thicknesses (i.e. t = 0.5, 1.0, and 2.0 mm) and three lengths (i.e. L_0 = 200, 250, and 300 mm) of the earth-retaining-wall model. L_0 is the embedded depth before excavation, which does not include the length of the protrusion above the ground.

DOI: 10.1201/9781003215226-36

Figure 1. Two types of aluminum rods.

Figure 2. Measurement of internal angle of friction (just before the aluminum rod collapsed).

Figure 3. Measurement of internal angle of friction (just after the aluminum rod collapsed).

The validity of modeling the earth-retaining-wall model was evaluated based on the product of the characteristic values β (Eq. 1) and L_0.

$$\beta = \sqrt[4]{\frac{k_h B}{4EI}} \tag{1}$$

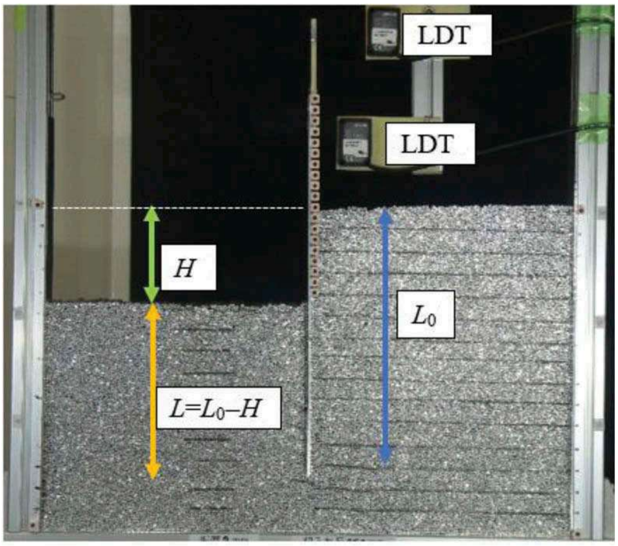

Figure 4. Layout of experimental apparatus.

where EI is the flexural rigidity of the earth-retaining-wall model, k_h is the coefficient of subgrade reaction, and B is the contact width between the ground and the earth-retaining-wall, which in this experiment is the aluminum rod's length (B=50mm).

This βL_0 value is a dimensionless parameter that represents the ratio of the rigidity of the wall relative to the ground. In other words, if modeled relative rigidity (βL_0) corresponds to that of an actual retaining wall, the model is considered valid.

To obtain the characteristic value β, the horizontal-loading test of each earth-retaining-wall model (Figure 5) was conducted separately prior to excavation. The value of β was calculated by applying Chang's equation (Eq. 2).

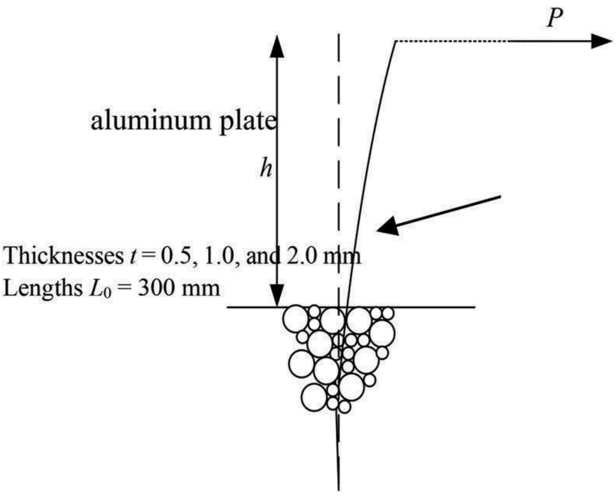

Figure 5. Horizontal loading test of the model earth retaining wall.

$$y_0 = \frac{P}{3EI\beta^3}\left\{(1 + h\beta)^3 + 1/2\right\} \quad (2)$$

where y_0 is the pile-head displacement; P is the horizontal load; h is the loading height.

The value of β was calculated backward for each earth-retaining-wall model from measured P and y_0 values shown in Figure 6. Table 1 presents the reciprocal of the measured characteristic value β of the pile and the value βL_0. This range of βL_0 values (i.e., 1.4–5.9) is wider than the general range of an actual cantilever-type earth-retaining wall, and the modeling of the wall in this experiment can be considered valid.

2.3 *Excavation*

The excavation was simulated step by step, removing and leveling the aluminum rods at a pitch of about 10 mm depth (Figure 7). At each excavation step, the horizontal displacement δ_0 of the earth-retaining-wall at the original ground surface height was measured. The horizontal displacement δ_0 was converted measured values of two laser displacement transducers (LDT, shown in Figure 4) at 40mm and 100mm height from the original ground surface of the protruding part of the earth retaining wall. The change in the unexcavated side ground's surface height due to excavation was not taken into account. However, if the range of LDT was exceeded, δ_0 was measured by tracking the reference point of the picture captured by a digital camera.

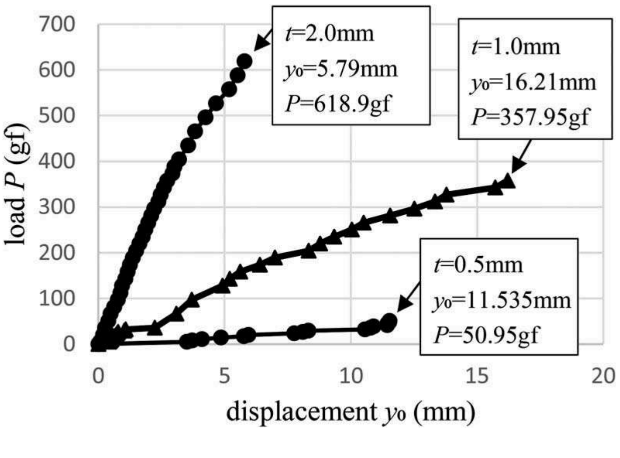

Figure 6. Horizontal loading test result.

Table 1. The characteristic value β of the pile.

Thickness	t = 0.5mm	t =1.0mm	t = 2.0mm
$1/\beta$	51mm	75mm	134mm
βL_0	3.9–5.9	2.7–4.0	1.4–2.2

Figure 7. A state of simulating excavation.

3 EXPERIMENTAL RESULT

Sample results are shown for cases 0.5 mm and 1.0 mm thickness, for the same length of the earth-retaining wall (i.e., L_0 = 200 mm).

Figure 8 shows the deformation of the ground model and the earth-retaining-wall model one step before collapse (excavation depth H = 110 mm for both). The point of collapse is the point at which passive collapse can be confirmed visually. The βL values shown in Figure 8 do not meet the criteria for semi-infinite length (generally $\beta L \geq$ 2.5–3.0), which is the principle of some design standards. When the

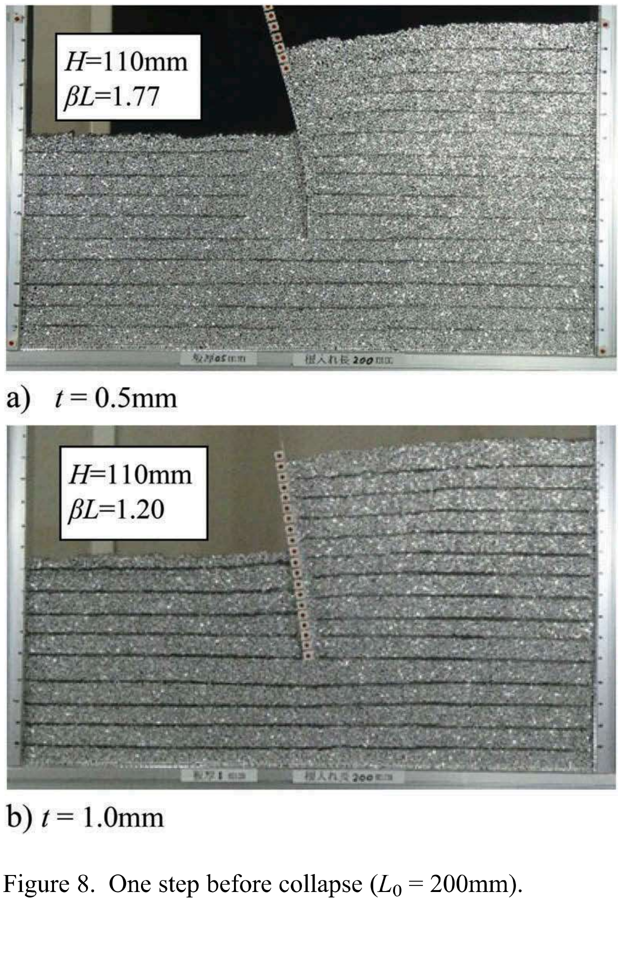

Figure 8. One step before collapse (L_0 = 200mm).

plate thickness was small (Figure 8a), the wall's deflection was significant. Conversely, when the plate thickness was large (Figure 8b), the wall was rigid (no deflection).

Figure 9 Shows the results for cases 0.5 mm and 1.0 mm for the same length L_0 (250 mm); i.e., only plate thickness was different for both cases. These figures indicate the behavior of the ground and wall models at the time of collapse (H = 140 mm). The dotted line in the figure indicates the visually confirmed slip surface. When the plate thickness is large (Figure 9b), the passive collapse is considerable, and the slip surface can be easily observed. In this case, when the plate thickness was small (Figure 9a), passive collapse did not occur, and a small slip surface could be observed near the wall model. Even at t = 2.0 mm, a significant slip surface (passive collapse) could be observed. From this, it was found that the ground's behavior on the excavation side is significantly affected by the rigidity of the earth-retaining wall.

Figure 10 shows the relationship between the excavation H_c at collapse and the plate thickness t during the collapse. It can be observed that H_c mainly depends on the retaining wall length L_0 and is hardly affected by rigidity.

Figure 11 shows the relationship between the excavation depth H and the horizontal displacement δ_0 of the earth retaining wall for all cases. Figure 12 shows the relationship between the horizontal displacement δ_0 and plate thickness t when excavation depth H was 50 mm. Figure 13 shows the relationship between the horizontal displacement δ_0 plate thickness t when H = 100 mm. Further, the effect of suppressing the horizontal displacement of the earth-retaining wall by increasing the embedded depth could not be verified; this effect was evaluated by increasing the plate thickness (flexural rigidity of the wall).

Therefore, from a perspective of displacement suppression, it was found that increasing the embedded depth had no effect on suppression, which solely depended only on the flexural rigidity of the retaining wall.

a) t=0.5mm b) t=1.0mm

Figure 9. Model earth retaining wall at the time of collapse.

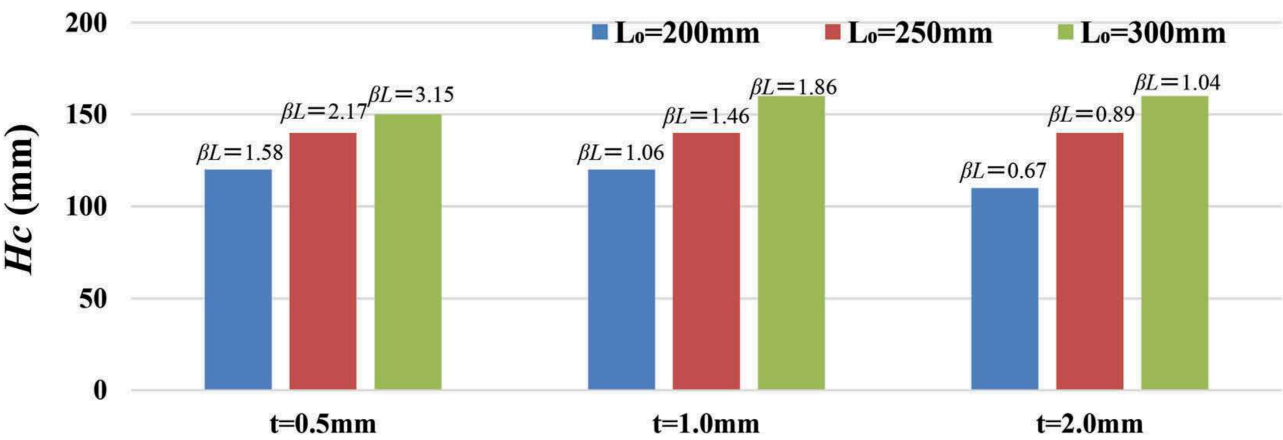

Figure 10. The relationship between the excavation depth H_c and plate thickness t during collapse.

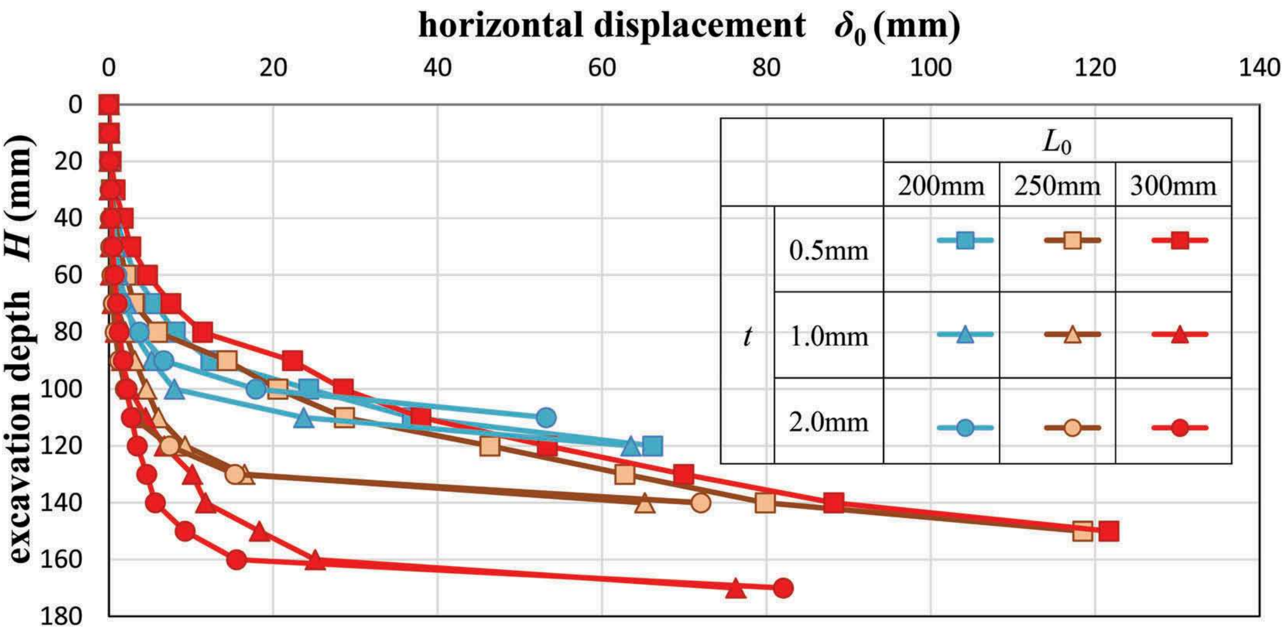

Figure 11. The relationship between the excavation depth H and the horizontal displacement δ_0 of the earth retain-ing wall in all cases.

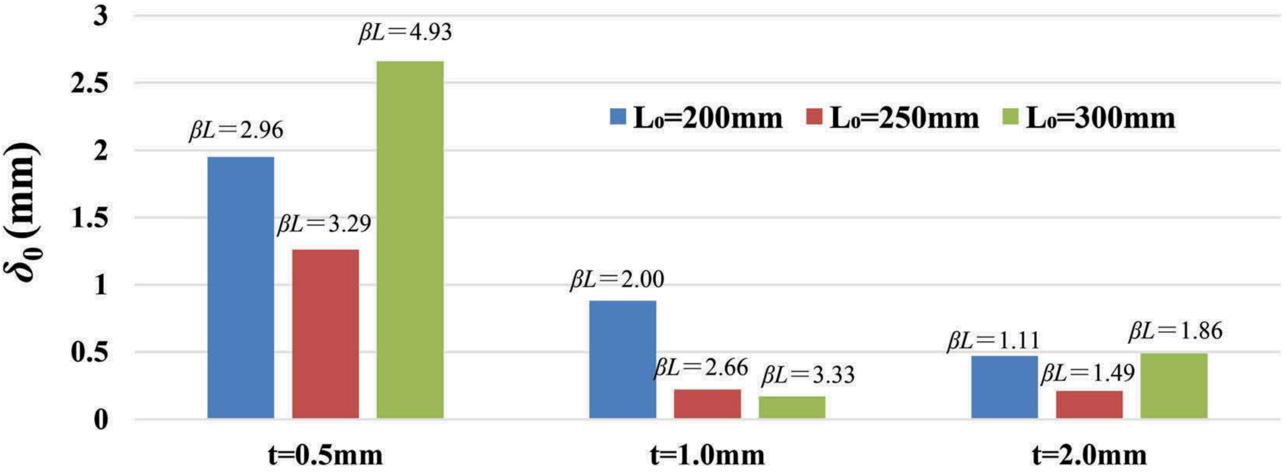

Figure 12. Relationship between horizontal displacement δ_0 and plate thickness t when the excavation depth H = 50 mm.

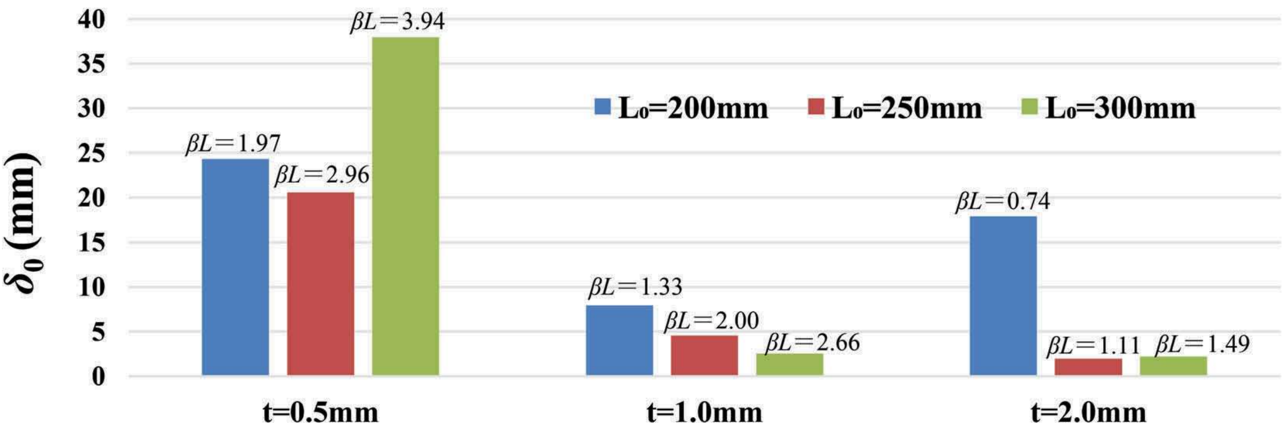

Figure 13. The relationship between the horizontal displacement δ_0 and plate thickness t when the excavation depth H = 100 mm.

4 COMPARISON WITH THEORETICAL VALUES

The horizontal displacement of the earth-retaining-wall model was compared with the experimental and theoretical values calculated using elasticity theory and Rankine's earth-pressure theory. The cantilever method (without bearings) can be obtained by using the Chang method, which is a general analysis that uses an elastic-bearing-beam model (simple beam-spring model) for designing foundation piles for horizontal forces (Figure 14). It should be noted that this theoretical value assumes that the earth-retaining wall is sufficiently deep and therefore semi-infinite, and that the ground at the embedded part is homogenous and isotropic.

The horizontal displacement of the earth retaining wall was calculated using Equation 3, where γ is weight per unit volume and φ is angle of internal friction.

$$\delta = \frac{Ph}{EI\beta^2}\left\{\frac{(1+\beta h)^3 1/2}{3\beta} + \frac{(1+\beta h)^2 l}{2}\right\} \tag{3}$$

$$P_h = 1/2 \times \gamma \times H^2 \times \tan^2(45^\circ - \varphi/2)$$

$$h = 1/3H$$

Figure 15 shows the relationship between the horizontal displacement obtained using the above equation and the horizontal displacement measured in the experiment for each plate thickness. A comparison of the horizontal displacement of t = 0.5 mm (Figure 15a) and the theoretical value from elasticity theory indicates that they are almost in agreement. However, the horizontal displacement of t = 2.0 mm (Figure 15c) deviates significantly from the theoretical value from elasticity theory as the excavation depth increases.

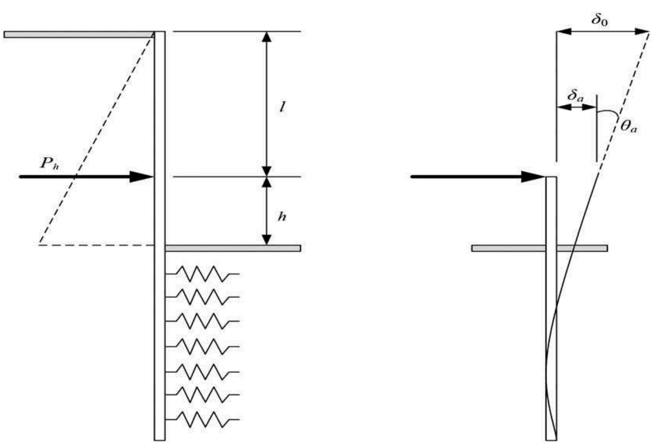

Figure 14. The Chang method.

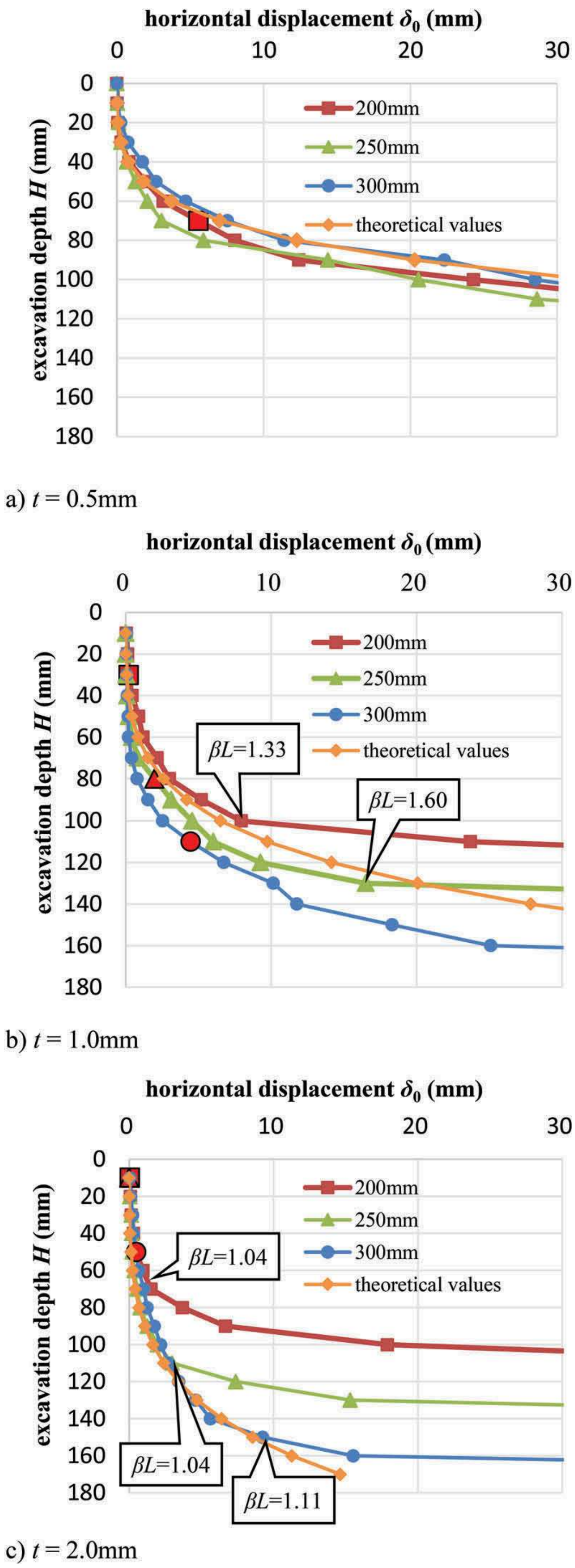

Figure 15. Comparison of experimental values and theoretical values.

In Figure 15, the depth (βL < 2.5), which cannot be regarded as semi-infinite, is plotted in red. As shown in the chart, even if this point is exceeded, the value initially approaches the theoretical value considered from the elasticity theory.

In addition, βL of the point at the excavation depth immediately before the displacement starts to increase; this trend deviates sharply from elasticity theory, as shown in the chart.

Notably, when βL = 1.0–1.6, the displacement of the elastic theory deviates. Hence, it is inferred from this observation that the displacement can be estimated by the theoretical value of elasticity theory if at least 1.0–1.6 is secured even if $\beta L \geq 2.5$ is not satisfied.

5 CONCLUSION

The results obtained from this study were as follows.

1) The decay depth of the earth-retaining wall does not depend on the wall's flexural rigidity; the flexural rigidity only affects the embedded depth. In addition, if the rigidity of the earth retaining wall is small, the extent of passive collapse (length of the slip face) becomes small as well.
2) The displacement-suppression effect of the earth-retaining wall during excavation was affected by the increase in the wall's flexural rigidity. In contrast, the effect of increasing the embedded depth on the wall's retaining capacity was not verified.
3) Even if the condition $\beta L \geq 2.5$ is not satisfied if $\beta L \geq 1.0$–1.6 is met, the displacement, which can be predicted from the theory of elasticity, does not deviate significantly.

In addition, the design standard $\beta L \geq 2.5$ is considered to cause the brittle failure of a highly rigid retaining wall. Consequently, the safety against collapse may be improved by increasing the embedded depth.

In the future, by clarifying the uncertainties to be considered and their effects, we would like to study a more reasonable and simple design method with an appropriate safety margin in a different way from $\beta L \geq 2.5$.

REFERENCES

Japanese Geotechnical Society: *Method for lateral load test of piles*, pp32 Maruzen Publishing, 2010. (in Japanese)

Japan Road Association: *Guidelines for Temporary structure of Road earth works*, pp153–154 Maruzen Publishing, 1994. (in Japanese)